Polymer 50 (2009) 613–626

Contents lists available at ScienceDirect

Polymer

journal homepage: www.elsevier.com/locate/polymer

Effect of phenol substitution on the network structure and properties of linear aliphatic diamine-based benzoxazines

Douglas J. Allen, Hatsuo Ishida*

Department of Macromolecular Science and Engineering, Case Western Reserve University, Cleveland, OH 44106-7202, United States

ARTICLE INFO

Article history:
Received 2 October 2008
Received in revised form
5 November 2008
Accepted 9 November 2008
Available online 17 November 2008

Keywrods:
Polybenzoxazine
Aliphatic diamine-based benzoxazine
Network structure

ABSTRACT

A series of aliphatic diamine-based benzoxazines with different phenolic substitutions have been synthesized and characterized. Molecular structure of the monomers is verified by ^{1}H and ^{13}C NMR, FTIR, and elemental analysis. The site of polymerization is regiospecified and the type of linkage in the network structure is manipulated by selectively blocking the *ortho*, *para*, and *meta* positions in the aromatic rings of the monomer. The controlled network structures and their properties are compared to those formed by the polymerization of aliphatic diamine-based benzoxazines prepared from unsubstituted phenol in order to provide insight into their structures. Investigation on the melting point, polymerization kinetics, gelation, and T_g and sub-T_g thermal transition is all reported on these systematically controlled structure polybenzoxazines.

© 2008 Elsevier Ltd. All rights reserved.

1. Introduction

Polybenzoxazines are a class of thermosetting phenolic resins that have recently been developed for the electronics, aerospace, and other industries as an attractive alternative to epoxies and traditional resole and novolac-type phenolic resins. Although the fundamental chemistry of benzoxazine monomers and early attempts to produce their oligomers and applications were reported many years ago [1,2], it was only in the last decade that the mechanical, physical, and chemical properties of polybenzoxazines have been discussed [3–11]. Benzoxazine monomers are readily synthesized, either in solution or with a melt state reaction, by the Mannich condensation of a phenolic derivative, formaldehyde, and a primary amine. Polymerization of a benzoxazine monomer occurs either with an initiator such as a phenol, or may be thermally activated. The advantages of benzoxazine resins and polybenzoxazines derived from those monomers are well documented in the literature [3–11].

The polybenzoxazines that dominate the literature are bisphenol-based, and thus achieve the polyfunctionality required to form an infinite network structure through synthesis utilizing a bifunctional phenolic molecule with a monofunctional amine. However, the wide variety of available phenolic precursors and primary amines allows for tremendous opportunities in molecular design and imparts the ability to tailor the structure for specific applications. This point is emphasized by the recent development of a series of low viscosity, diamine-based benzoxazine monomers. These monomers were synthesized using a monofunctional phenol rather than a bisphenol, but with a linear aliphatic diamine to provide polyfunctionality. The properties of these diamine-based polybenzoxazines were tailored by varying the length of the linear aliphatic chain during synthesis. The diamine-based benzoxazines with a two carbon aliphatic chain demonstrated the ability to polymerize rapidly at temperatures lower than typical benzoxazines, while maintaining a comparable glass transition temperature and improved mechanical properties. Synthesis with longer aliphatic chains, containing between four and twelve carbons, produced inherently flexible polybenzoxazines with flexural strains at break as high as 12%, yet retaining reasonable thermal properties.

In earlier work, Burke et al. [1] qualitatively observed that the polymerization reaction of benzoxazines preferentially occurred at the *ortho* rather than the *para* or *meta* positions of the phenol. Riess and coworkers [12] confirmed this regioselectivity in model compounds as they followed the kinetics of polymerization for thermally activated and substituted-phenol initiated monofunctional benzoxazines. However, their results clearly demonstrated that a reaction at the *para* position is possible, albeit with a higher activation energy and lower rate of reaction than the *ortho* position. Other researchers have indicated that the *meta* positions of the aromatic ring can also be reactive during polymerization of benzoxazines at high temperatures and/or very long polymerization times [13]. In the previously described research on aliphatic diamine-

* Corresponding author. Department of Macromolecular Science and Engineering, Case Western Reserve University, 10900 Euclid Avenue, Cleveland, OH 44106-7202, United States.
E-mail address: hxi3@cwru.edu (H. Ishida).

0032-3861/$ – see front matter © 2008 Elsevier Ltd. All rights reserved.
doi:10.1016/j.polymer.2008.11.007

based polybenzoxazines, the *ortho* position of the phenol was assumed to be the preferred site for polymerization. The possibilities of polymerization occurring at the open *para*- or *meta*-position in addition to the *ortho* position, and the potential contribution of a reaction at these sites to the overall polymer structure and properties were not formally investigated, but only casually discussed. In this work, benzoxazines will be synthesized from methyl-substituted phenols, in which an *ortho*, *meta*, or *para* position of the phenol is systematically blocked in order to regiospecify the reaction site during polymerization. As demonstrated in Fig. 1, blocking the *para* position will force the formation of polybenzoxazine network structure containing only *ortho–ortho* linkages, while blocking the *ortho* position of the phenol will necessitate the formation of a network consisting entirely of *ortho–para* linkages. These controlled network structures will then be compared to that formed from the polymerization of aliphatic diamine-based benzoxazines prepared from unsubstituted phenol. Without blocked reaction sites, the phenol-based polybenzoxazine network structure is expected to contain a mixture of both *ortho–ortho* and *ortho–para* linkages, perhaps with some individual phenol groups reacting at both the *ortho* and the *para* positions. Thus, in the following study, the effects of phenol substitution, as well as aliphatic diamine chain length, on the rate of polymerization, thermal behavior, and network properties will be extensively investigated.

2. Experimental

2.1. Materials

Phenol (99%) and 1,6-hexadiamine (99.5%) (ad6) were purchased from the Acros Division of Fisher Scientific. Ethylene diamine (99%) (ad2), *o*-cresol (99%), *p*-cresol (99%), *m*-cresol (99%), and paraformaldehyde (95%) were obtained from Aldrich Chemical, while 1,12-diaminododecane (99%) (ad12) was purchased from Fluka. All chemicals were used as received with no further purification.

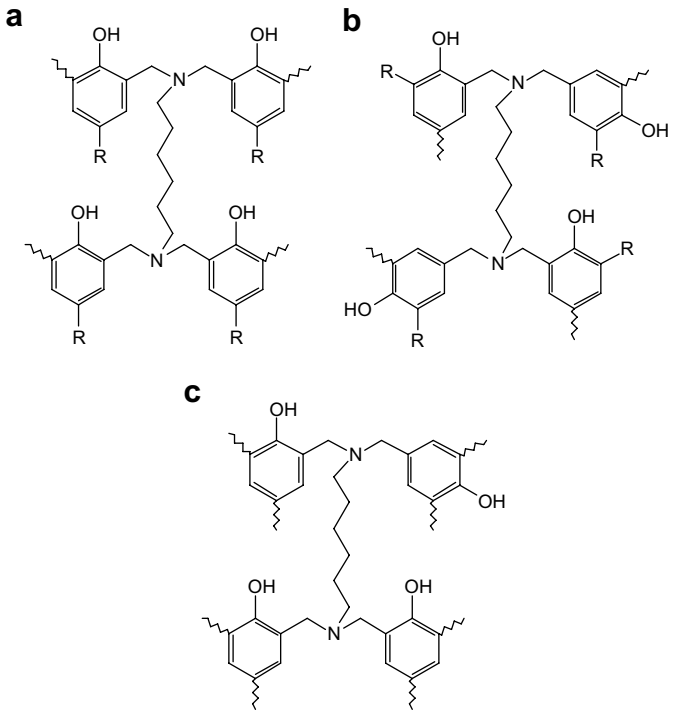

Fig. 1. Model polybenzoxazine network structures based on a (a) *para*-substituted monomer, (b) *ortho*-substituted monomers, and (c) unsubstituted monomer.

2.2. Synthesis of benzoxazine monomers

The solventless synthesis method, detailed elsewhere [14], was modified for the synthesis of each difunctional, aliphatic diamine-based benzoxazine monomer. Phenol, paraformaldehyde, and aliphatic diamine were dry mixed in the stoichiometric amounts (2:4:1) in a single neck reaction flask. Approximately 5 ml of chloroform per gram of reactants were added to the flask. The reaction mixture was refluxed with stirring for a time period between 1.5 and 12 h as specified for each monomer in Table 1. Optimization of reaction time was made for each material. After cooling to room temperature, the crude reaction products were washed several times with 1 N NaOH solution and then rinsed with distilled water until neutral. The base washed products were dried over sodium sulfate and filtered, followed by solvent removal under vacuum. The material was further purified by rinsing with the alcohol as indicated in Table 1. The purified benzoxazine monomer was dried under vacuum at room temperature for 24 h and refrigerated until the time of use. Successful synthesis and purity were verified by NMR and FTIR spectroscopies.

Ethylene diamine-based benzoxazine monomer, 1,2-bis(3,4-dihydro-2*H*-1,3-benzoxazin-3-yl) ethane; 1,6-hexadiamine-based benzoxazine monomer, 1,6-bis(3,4-dihydro-2*H*-1,3-benzoxazin-3-yl) hexane ethane; and 1,12-diaminododecane-based benzoxazine monomer, 1,12-bis(3,4-dihydro-2*H*-1,3-benzoxazin-3-yl) dodecane were synthesized according to the above procedure, utilizing a 1.5, 8 and 12 h reaction period, respectively, and methanol as the wash alcohol. All materials were white powder. Analysis results of the above three benzoxazines were reported elsewhere [15]. Only the newly synthesized compounds in this study will be described below.

o-Cresol/ethylene diamine-based benzoxazine monomer. 1,2-Bis(8-methyl-3,4-dihydro-2*H*-1,3-benzoxazin-3-yl) ethane was synthesized according to the above procedure, utilizing a 1.5 h reaction period and methanol as the wash alcohol. White powder.

^{1}H NMR ($CDCl_3$, 200 MHz ^{1}H, 298 K, δ): 2.17 (6H, Ar–CH_3), 2.97 (4H, N–CH_2–CH_2), 4.03 (4H, Ar–CH_2–N), 4.93 (4H, O–CH_2–N), 6.73–7.00 (6H, Ar–H).

^{13}C NMR ($CDCl_3$, 50.3 MHz ^{13}C, 298 K, δ): 15.55 (2C, C–Ar), 49.49 (2C, N–C–C), 50.42 (2C, Ar–C–N), 82.70 (2C, O–C–N), 119.23 (2C, Ar), 119.78 (2C, Ar), 124.95 (2C, Ar), 125.48 (2C, Ar), 128.78 (2C, Ar), 152.20 (2C, Ar).

p-Cresol/ethylene diamine-based benzoxazine monomer. 1,2-Bis(6-methyl-3,4-dihydro-2*H*-1,3-benzoxazin-3-yl) ethane was synthesized according to the above procedure, utilizing a 1.5 h reaction period and methanol as the wash alcohol. White powder.

^{1}H NMR ($CDCl_3$, 200 MHz ^{1}H, 298 K, δ): 2.24 (6H, Ar–CH_3), 2.96 (4H, N–CH_2–CH_2), 4.00 (4H, Ar–CH_2–N), 4.87 (4H, O–CH_2–N), 6.65–6.95 (6H, Ar–H).

^{13}C NMR ($CDCl_3$, 50.3 MHz ^{13}C, 298 K, δ): 20.53 (2C, C–Ar), 49.48 (2C, N–C–C), 50.29 (2C, Ar–C–N), 82.59 (2C, O–C–N), 116.09 (2C, Ar), 119.56 (2C, Ar), 127.81 (2C, Ar), 128.24 (2C, Ar), 129.72 (2C, Ar), 151.79 (2C, Ar).

m-Cresol/ethylene diamine-based benzoxazine monomer. 1,2-Bis(7-methyl-3,4-dihydro-2*H*-1,3-benzoxazin-3-yl) ethane was

Table 1
Nomenclature, reaction times, and type of alcohol wash used in the synthesis of the linear aliphatic diamine-based benzoxazine monomers.

Monomer	Diamine	Reaction time (h)	Wash alcohol	Molecular weight
P-ad2	Ethylene diamine	1.5	Methanol	296.36
P-ad4	1,4-Diaminobutane	4	Methanol	324.42
P-ad6	1,6-Hexane diamine	8	1-Butanol	352.47
P-ad8	1,8-Diaminooctane	10	1-Butanol	380.52
P-ad12	1,12-Diaminododecane	12	1-Butanol	436.63

synthesized according to the above procedure, utilizing a 1.5 h reaction period and methanol as the wash alcohol. White powder.

^{1}H NMR ($CDCl_3$, 200 MHz ^{1}H, 298 K, δ): 2.28 (6H, Ar–CH_3), 2.96 (4H, N–CH_2–CH_2), 4.00 (4H, Ar–CH_2–N), 4.88 (4H, O–CH_2–N), 6.60–6.85 (6H, Ar–H).

^{13}C NMR ($CDCl_3$, 50.3 MHz ^{13}C, 298 K, δ): 49.51 (2C, N–C–C), 50.31 (2C, Ar–C–N), 82.64 (2C, O–C–N), 116.36 (2C, Ar), 119.91 (2C, Ar), 120.51 (2C, Ar), 127.50 (2C, Ar), 127.68 (2C, Ar), 154.06 (2C, Ar).

o-Cresol/1,6-hexadiamine-based benzoxazine monomer. 1,6-Bis(8-methyl-3,4-dihydro-2*H*-1,3-benzoxazin-3-yl) hexane ethane was synthesized according to the above procedure, utilizing an 8 h reaction period and 1-butanol as the wash alcohol. White powder.

^{1}H NMR ($CDCl_3$, 200 MHz, 298 K, δ): 1.36, 1.56 (8H, CH_2–CH_2–CH_2), 2.17 (6H, Ar–CH_3), 2.69, 2.71, 2.74 (4H, N–CH_2–CH_2), 3.96 (4H, Ar–CH_2–N), 4.87 (4H, O–CH_2–N), 6.73–6.99 (6H, Ar–H).

^{13}C NMR ($CDCl_3$, 50.3 MHz ^{13}C, 298 K, δ): 15.56 (2C, C–Ar), 27.09 (2C, C–C–C), 28.06 (2C, C–C–C), 50.30 (2C, Ar–C–N), 51.29 (2C, N–C–C), 82.47 (2C, O–C–N), 119.50 (2C, Ar), 119.66 (2C, Ar), 124.90 (2C, Ar), 125.39 (2C, Ar), 128.67 (2C, Ar), 152.27 (2C, Ar).

p-Cresol/1,6-Hexadiamine-based Benzoxazine Monomer. 1,6-Bis(6-methyl-3,4-dihydro-*2H*-1,3-benzoxazin-3-yl) hexane ethane was synthesized according to the above procedure, utilizing an 8 h reaction period and 1-butanol as the wash alcohol. White powder.

^{1}H NMR ($CDCl_3$, 200 MHz, 298 K, δ): 1.34, 1.55 (8H, CH_2–CH_2–CH_2), 2.24 (6H, Ar–CH_3), 2.69, 2.72, 2.74 (4H, N–CH_2–CH_2), 3.93 (4H, Ar–CH_2–N), 4.82 (4H, O–CH_2–N), 6.64–6.92 (6H, Ar–H).

^{13}C NMR ($CDCl_3$, 50.3 MHz ^{13}C, 298 K, δ): 20.54 (2C, C–Ar), 27.07 (2C, C–C–C), 28.03 (2C, C–C–C), 50.11 (2C, Ar–C–N), 51.22 (2C, N–C–C), 82.31 (2C, O–C–N), 116.01 (2C, Ar), 119.82 (2C, Ar), 127.79 (2C, Ar), 128.13 (2C, Ar), 129.58 (2C, Ar), 151.87 (2C, Ar).

m-Cresol/1,6-hexadiamine-based benzoxazine monomer. 1,6-Bis(7-methyl-3,4-dihydro-2*H*-1,3-benzoxazin-3-yl) hexane ethane was synthesized according to the above procedure, utilizing an 8 h reaction period and 1-butanol as the wash alcohol. White powder.

^{1}H NMR ($CDCl_3$, 200 MHz, 298 K, δ): 1.34, 1.55 (8H, CH_2–CH_2–CH_2), 2.27 (6H, Ar–CH_3), 2.67, 2.71, 2.75 (4H, N–CH_2–CH_2), 3.94 (4H, Ar–CH_2–N), 4.83 (4H, O–CH_2–N), 6.59–6.85 (6H, Ar–H).

^{13}C NMR ($CDCl_3$, 50.3 MHz ^{13}C, 298 K, δ): 27.05 (2C, C–C–C), 28.00 (2C, C–C–C), 50.17 (2C, Ar–C–N), 51.22 (2C, N–C–C), 82.37 (2C, O–C–N), 116.27 (2C, Ar), 120.19 (2C, Ar), 120.38 (2C, Ar), 127.47 (2C, Ar), 127.56 (2C, Ar), 154.14 (2C, Ar).

o-Cresol/1,12-diaminododecane-based benzoxazine monomer. 1,12-Bis(8-methyl-3,4-dihydro-2*H*-1,3-benzoxazin-3-yl) dodecane was synthesized according to the above procedure, utilizing a 12 h reaction period and 1-butanol as the wash alcohol. White powder.

^{1}H NMR ($CDCl_3$, 200 MHz, 298 K, δ): 1.25 (16H, CH_2–CH_2–CH_2), 1.55 (4H, CH_2–CH_2–CH_2), 2.17 (6H, Ar–CH_3), 2.69, 2.71, 2.74 (4H, N–CH_2–CH_2), 3.97 (4H, Ar–CH_2–N), 4.87 (4H, O–CH_2–N), 6.75–6.98 (4H, Ar–H).

^{13}C NMR ($CDCl_3$, 50.3 MHz ^{13}C, 298 K, δ): 27.20 (2C, C–C–C), 28.11 (2C, C–C–C), 29.47 (2C, C–C–C), 29.52 (2C, C–C–C), 29.54 (2C, C–C–C), 50.22 (2C, Ar–C–N), 51.36 (2C, N–C–C), 82.39 (2C, O–C–N), 116.28 (2C, Ar), 120.26 (2C, Ar), 120.36 (2C, Ar), 127.48 (2C, Ar), 127.55 (2C, Ar), 154.18 (2C, Ar).

p-Cresol/1,12-diaminododecane-based benzoxazine monomer. 1,12-Bis(6-methyl-3,4-dihydro-2*H*-1,3-benzoxazin-3-yl) dodecane was synthesized according to the above procedure, utilizing a 12 h reaction period and 1-butanol as the wash alcohol. White powder.

^{1}H NMR ($CDCl_3$, 200 MHz, 298 K, δ): 1.25 (16H, CH_2–CH_2–CH_2), 1.54 (4H, CH_2–CH_2–CH_2), 2.24 (6H, Ar–CH_3), 2.69, 2.72, 2.74 (4H, N–CH_2–CH_2), 3.94 (4H, Ar–CH_2–N), 4.83 (4H, O–CH_2–N), 6.65–6.92 (6H, Ar–H).

^{13}C NMR ($CDCl_3$, 50.3 MHz ^{13}C, 298 K, δ): 27.20 (2C, C–C–C), 28.11 (2C, C–C–C), 29.47 (2C, C–C–C), 29.52 (2C, C–C–C), 29.54 (2C, C–C–C), 50.22 (2C, Ar–C–N), 51.36 (2C, N–C–C), 82.39 (2C, O–C–N), 116.28 (2C, Ar), 120.26 (2C, Ar), 120.36 (2C, Ar), 127.48 (2C, Ar), 127.55 (2C, Ar), 154.18 (2C, Ar).

m-Cresol/1,12-diaminododecane-based benzoxazine monomer. 1,12-Bis(7-methyl-3,4-dihydro-2*H*-1,3-benzoxazin-3-yl) dodecane was synthesized according to the above procedure, utilizing a 12 h reaction period and 1-butanol as the wash alcohol. White powder.

^{1}H NMR ($CDCl_3$, 200 MHz, 298 K, δ): 1.25 (16H, CH_2–CH_2–CH_2), 1.54 (4H, CH_2–CH_2–CH_2), 2.27 (6H, Ar–CH_3), 2.68, 2.72, 2.75 (4H, N–CH_2–CH_2), 3.95 (4H, Ar–CH_2–N), 4.84 (4H, O–CH_2–N), 6.60–6.85 (6H, Ar–H).

^{13}C NMR ($CDCl_3$, 50.3 MHz ^{13}C, 298 K, δ): 27.20 (2C, C–C–C), 28.11 (2C, C–C–C), 29.47 (2C, C–C–C), 29.52 (2C, C–C–C), 29.54 (2C, C–C–C), 50.22 (2C, Ar–C–N), 51.36 (2C, N–C–C), 82.39 (2C, O–C–N), 116.28 (2C, Ar), 120.26 (2C, Ar), 120.36 (2C, Ar), 127.48 (2C, Ar), 127.55 (2C, Ar), 154.18 (2C, Ar).

2.3. NMR

The structures of the diamine-based benzoxazine monomers were verified by both proton (^{1}H) and carbon (^{13}C) nuclear magnetic resonance (NMR) spectroscopies utilizing a Varian Gemini XL-200 spectrometer operating at a proton frequency of 200 MHz and the corresponding carbon frequency. Monomers were dissolved in deuterated chloroform with all peaks referenced relative to tetramethylsilane (TMS). Proton spectra were obtained using 64 transients and a concentration of 1 wt%, while 1024 transients and a concentration of 5 wt% were used for the ^{13}C spectra.

2.4. Fourier transform infrared spectroscopy

Fourier transform infrared (FTIR) spectra of the benzoxazine monomers and polymers were obtained on a Biorad FTS-60A spectrometer with a potassium bromide (KBr) beamsplitter and a deuterated triglycine sulfate (DTGS) detector. The spectrometer was purged with dry nitrogen and operated in transmission mode utilizing the co-addition of 128 scans at a resolution of 2 cm^{-1}. The monomer spectra were obtained from 1–2 mg samples cast from chloroform onto 25 mm KBr plates.

FTIR spectroscopy was also utilized to follow the polymerization of each monomer at 180 °C. The kinetic spectra were obtained using the same spectrometer fitted with a Connecticut Instruments hot cell in which the samples could be heated rapidly and held to within a degree of the set temperature. To minimize thickness changes due to flow, thin films of the benzoxazine monomers were sandwiched between two 20 mm KBr plates. The samples were heated and allowed to stabilize at 120 °C, which will later be shown to be above the melting point of most of the monomers but low enough to prevent any significant reaction. After thickness appeared to be constant, the cell was rapidly heated at a rate of approximately 30 °C/min. Data acquisition was initiated immediately upon reaching the 180 °C polymerization temperature. Win-IR Pro kinetic software permitted continuous scanning at a resolution of 2 cm^{-1} with spectral sets of 33 co-added scans stored every minute for the duration of each 150 min polymerization cycle. A 128 scan, room temperature FTIR spectrum of each polymer was also taken after the cell had fully cooled at the end of each kinetic experiment.

2.5. Differential scanning calorimetry

The melting points and reaction exotherms of the benzoxazine monomers were measured via differential scanning calorimetry (DSC) utilizing a TA Instruments DSC 2910 calorimeter equipped with a Pressure DSC cell. Thermal data analysis was performed using TA Instruments Universal Analysis software. Benzoxazine

samples of approximately 4 mg were scanned in hermetic aluminum sample pans with pierced upper lids. Thermograms were obtained at a heating rate of 10 °C/min over a temperature range of 25–300 °C with the DSC cell pressurized by nitrogen to 2.8 MPa. Curve resolving was performed in Grams/32 software (Galactic Industries) using a mixed Gaussian–Lorentzian function until convergence of least-squares curve fitting.

2.6. Chemorheology

Rheological analysis during the polymerization of the aliphatic diamine-based benzoxazines was performed utilizing a Rheometrics Dynamic Mechanical Spectrometer (RMS-800) equipped with a 2000/200 g cm dual-range force rebalance transducer set for the high range. A forced air convection oven surrounded the test fixture, allowing the temperature to be controlled at 180 °C to better than ±0.2 °C. Samples were subjected to dynamic shear in 25-mm or 40-mm parallel plate geometry using disposable aluminum plates. The evolution of rheological properties during polymerization for each of the different benzoxazine monomers was measured at a frequency of 1 Hz (6.28 rad/s) and a time resolution of 10 s. Polymerizing aliphatic diamine benzoxazine samples were contained within a 1 mm gap between the parallel plates and subjected to a sinusoidal strain of 3%.

2.7. Dynamic mechanical analysis

Dynamic mechanical spectra were also obtained from the above-described dynamic mechanical spectrometer. Specimens with dimensions of approximately 50 × 12.5 × 3 mm were tested in a rectangular torsion fixture. A sinusoidal shear strain of 0.1% was applied at a frequency of 1 Hz during each temperature sweep experiment. Linearity of the chosen shear strain was verified by a strain sweep prior to each experiment. Measurements were collected every 2 °C as the samples were heated at a rate of approximately 2 °C/min from −150 °C to well above the glass transition of each material.

2.8. Thermogravimetric analysis

The thermal stability of the aliphatic diamine-based benzoxazines was measured by thermogravimetric analysis (TGA) using a TA Instruments High Resolution 2950 Thermogravimetric Analyzer equipped with an evolved gas analysis (EGA) furnace. Weight loss was monitored as 20 mg samples were heated at a rate of 20 °C/min to a maximum temperature of 800 °C under a 90 ml/min dry nitrogen purge.

3. Results and discussion

In order to investigate the effect of phenol substitution and regioselectivity of the benzoxazine polymerization reaction on the polybenzoxazine network structure and properties, a series of twelve different linear aliphatic diamine-based benzoxazine monomers were synthesized and characterized. This series of monomers is shown in Fig. 2 along with the nomenclature that will be used for each compound throughout the paper. In addition to the unsubstituted, phenol-based compounds investigated previously, this series also includes monomers substituted by a single methyl group at the *ortho*, *para*, or *meta* position. For each different type of substitution, three different aliphatic diamine chain lengths were investigated ($n = 2, 6, 12$).

Idealized network structures for the polybenzoxazines prepared from the unsubstituted, *ortho*, and *para*-substituted monomers are shown in Fig. 1. The unsubstituted phenol-based benzoxazines can theoretically polymerize through either the free *ortho* or *para* position of the phenol, and thus should contain a mixture of two different types of linkages, *ortho–ortho* and *ortho–para*. By preparing monomers from *p*-cresol, the *para* position of the phenol can be blocked by a methyl substituent to force polymerization to occur only through the free *ortho* position. Unlike the unsubstituted compounds, the network structure of the *para*-substituted polybenzoxazines should be uniformly comprised of *ortho–ortho* linkages. Conversely, the blocked position of the *ortho*-substituted compounds should yield polybenzoxazines with only *ortho–para* linkages. It is anticipated that through the characterization of the controlled network structures, this research will be able to elucidate the contributions of the *ortho* and *para* reactive sites to the overall properties of the phenol-based diamine polybenzoxazines.

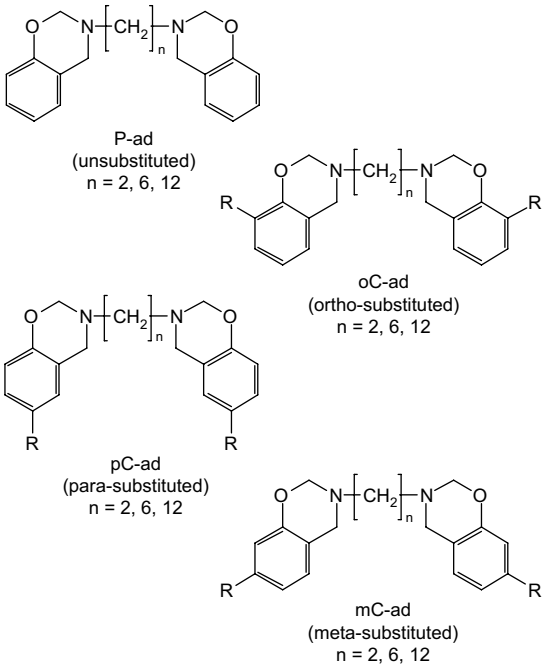

Fig. 2. Benzoxazine monomers synthesized in order to study the effect of phenol substitution on the polymer network structure and properties.

3.1. NMR analysis of monomer

Both NMR and FTIR spectroscopies confirmed the structure of the substituted linear aliphatic diamine-based benzoxazine monomers. The proton NMR spectra for the series of diamine-based benzoxazines are shown in Fig. 3. Only the spectra of ethylene diamine-based benzoxazine series are shown as representative examples. Each spectrum shows two peaks, centered at approximately 4.0 and 4.9 ppm, which are consistent with the formation of a benzoxazine ring [3]. The Mannich bridge protons of open oxazine rings are typically located at approximately 3.7 ppm and thus the absence of any proton peaks in this region indicates that the alcohol washes were successful at separating any oligomeric species from the monomers. Integration analysis of the proton peaks shows the closed-ring content of each compound to be better than 98%.

3.2. Infrared analysis of monomer

As would be expected, the infrared spectra of the benzoxazine monomers within each substitution group are very similar throughout the fingerprint region regardless of diamine chain length. There are a number of infrared bands in the spectra,

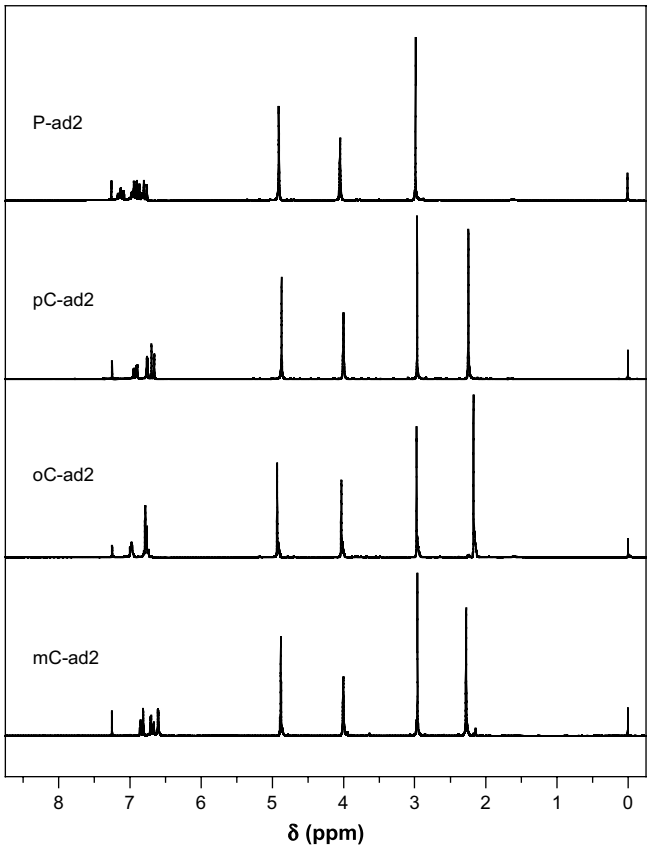

Fig. 3. Proton NMR spectra for the benzoxazine monomers derived from ethylene diamine.

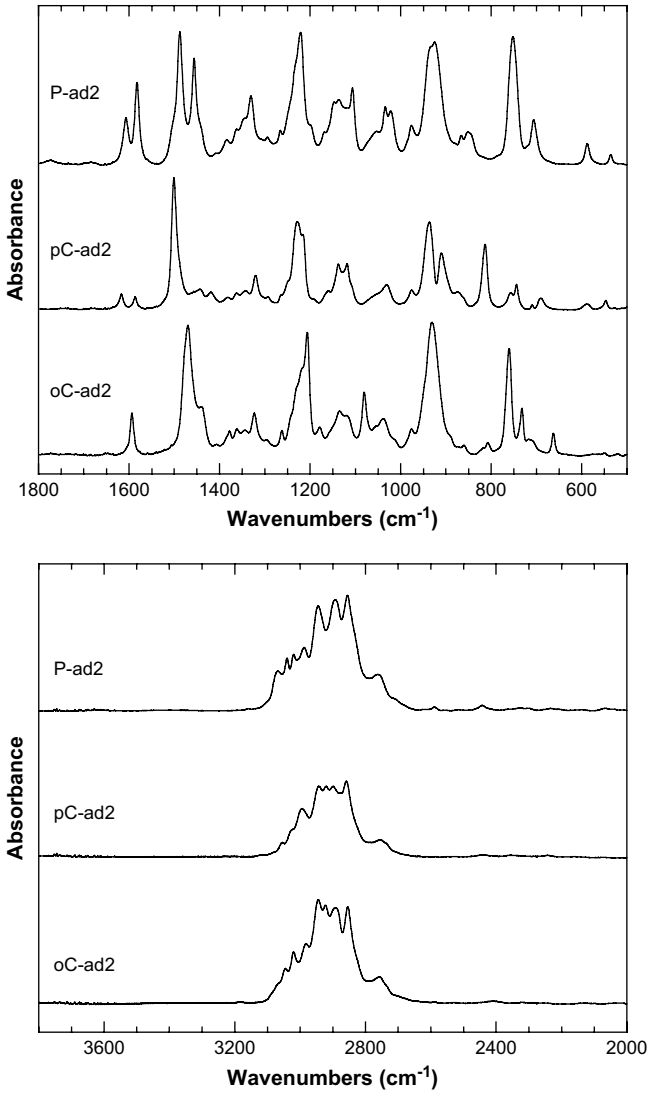

Fig. 4. Infrared spectra for the fingerprint (top) and hydroxyl regions (bottom) of the unsubstituted, *para*-substituted, and *ortho*-substituted monomers based on ethylene diamine.

highlighted in Fig. 4, which can be used to verify the formation of oxazine rings in each monomer. Similar to the NMR spectra, only the spectra of ethylene diamine-based benzoxazine series are shown as representative spectra. The presence of the benzoxazine ring aromatic ether is confirmed by an absorbance peak centered between 1030 and 1040 cm^{-1} due to the C–O–C symmetric stretching mode, and also between 1221 and 1228 cm^{-1} for the asymmetric stretching modes, regardless of substitution [10]. Characteristic modes of benzene with an attached oxazine ring are located at 925 cm^{-1} and 934 cm^{-1} for the phenol-based monomers, at 911 cm^{-1} and 937 cm^{-1} for the *p*-cresol based monomers, and between 927 and 932 cm^{-1} for the *o*-cresol based benzoxazine monomers [16]. There are also a number of other substitution specific benzene modes that can further confirm the monomer structure. For the phenol-based benzoxazine monomers, absorption bands characteristic of *ortho*-disubstituted benzene [17] appear at 1607 and 1583 cm^{-1}, 1488 and 1457 cm^{-1}, as well as 752 cm^{-1}. Peaks characteristic of asymmetric trisubstituted benzene appear in the *p*-cresol based monomers at 1617 and 1587 cm^{-1}, 1501 cm^{-1}, and finally 874 (weak) and 814 cm^{-1} (strong). The vicinal trisubstituted benzene modes appearing around 1595 cm^{-1}, 1470 cm^{-1}, 761 cm^{-1} (strong) and 734 cm^{-1} (weak) aid in confirming the successful synthesis of the *o*-cresol based benzoxazine monomers.

3.3. Differential scanning calorimetry

The effect of phenol substitution on the thermally activated polymerization behavior of the aliphatic diamine-based benzoxazine series was studied by differential scanning calorimetry with the results summarized in Table 2. The non-isothermal polymerization thermograms of the ethylene diamine-based (ad2) monomers are plotted in Fig. 5, while those for the diaminohexane (ad6) group are shown in Fig. 6. Exothermic behaviors of diaminododecane (ad12) are nearly identical to diaminohexane

Table 2
Results of the DSC analysis of the substituted, linear aliphatic diamine-based series of benzoxazines.

Monomer	Melting temperature (°C)	Exotherm position (°C)	MW (g/mol)	Exotherm (J/g)	Normalized exotherm (kJ/mol)
P-ad2	112.0	185.2	296.36	444	132
pC-ad2	117.9	192.8	324.42	316	103
oC-ad2	140.1	233.7	324.42	317	103
mC-ad2	169.4	196.7	324.42	321	104
P-ad6	83.3	224.9	352.47	292	103
pC-ad6	75.5	244.2	380.52	253	96
oC-ad6	99.6	249.9	380.52	250	95
mC-ad6	121.9	238.1	380.52	261	99
P-ad12	48.9	241.3	436.63	229	100
pC-ad12	72.2	250.0	464.68	217	101
oC-ad12	57.4	262.1	464.68	215	100
mC-ad12	79.1	249.9	464.68	220	102

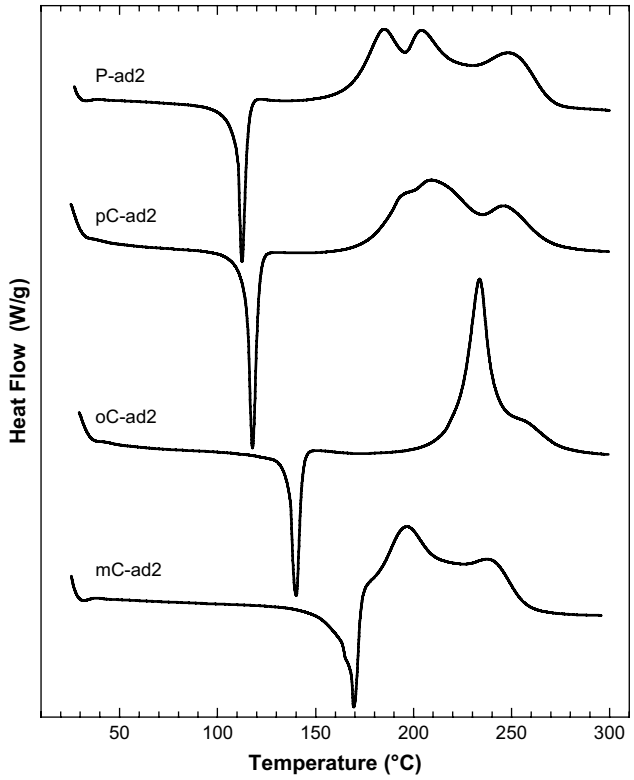

Fig. 5. Non-isothermal DSC thermograms of the unsubstituted, *para*-substituted, *ortho*-substituted and *meta*-substituted monomers based on ethylene diamine.

(ad6)-based benzoxazines, and, thus, they are not shown. As can be seen from the summarized data in Fig. 7, the melting point of the benzoxazine monomers is greatly affected by both phenol substitution and diamine chain length. In general, adding a methyl

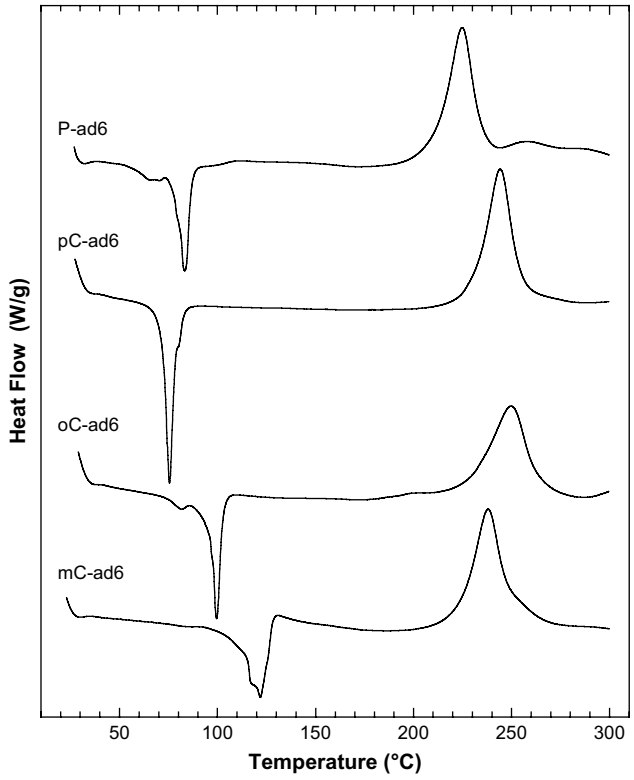

Fig. 6. Non-isothermal DSC thermograms of the unsubstituted, *para*-substituted, *ortho*-substituted and *meta*-substituted monomers based on diaminohexane.

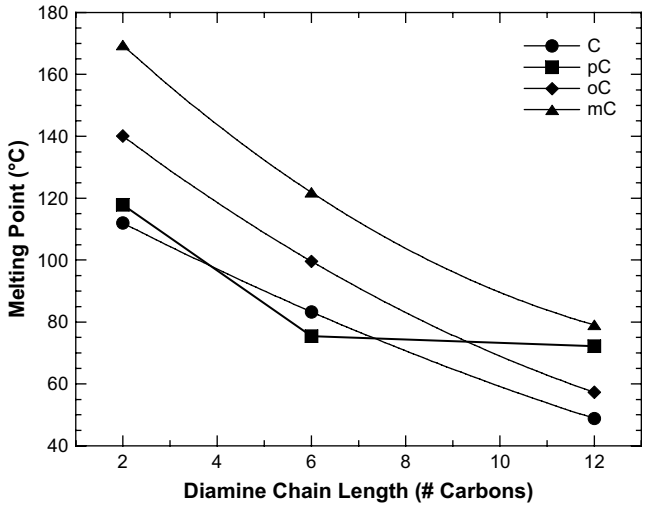

Fig. 7. Effect of phenol substitution and aliphatic diamine chain length on the melting point of the benzoxazine monomers.

substituent to the phenol appears to increase the position of the benzoxazine melting endotherm, with *meta*-substituted monomers yielding melting temperatures more than 20 °C higher than *ortho*-substituted monomers, and at least 30 °C higher than unsubstituted compounds. Regardless of substitution, the melting temperatures of the linear aliphatic diamine-based series of monomers decrease as a function of diamine chain length. The longest chain, *p*-cresol based compound, pC-ad12, exhibits somewhat anomalous behavior in that the position of its melting endotherm is almost identical to that of the middle chain length compound, pC-ad6, and is within a few degrees of the *meta*-substituted ad12 compound.

Inspection of the DSC polymerization exotherms for the ethylene diamine (ad2) based series benzoxazine monomers reveals that these compounds are unique in that they are each comprised of several overlapped peaks. Both P-ad2 and pC-ad2 appear to have three separate processes contributing to the overall polymerization exotherm, while oC-ad2 and mC-ad2 each have two overlapped exothermic peaks. Later results will show that the polybenzoxazines prepared from these monomers have a somewhat lower thermal stability than the longer diamine chain compounds, and thus it can be assumed that degradation rather than polymerization is responsible for the highest temperature peak in each of these exotherms. The two overlapped exotherm peaks of P-ad2 and pC-ad2 are centered at temperatures that are atypically low for benzoxazines. Previous work [18] suggests that this dual-mode process may be the product of the very short ethane linkage allowing steric hindrance or other structural factors and interactions to destabilize the oxazine rings and allow polymerization at lower temperatures.

From Fig. 8, it is apparent that for each group of similar phenol substitution, the temperature required to thermally activate benzoxazine polymerization directly increases as a function of diamine chain length. The shortest diamine chain monomers, with the exception of oC-ad2, undergo polymerization quite readily without an external initiator or catalyst as is demonstrated by onset temperatures 30–60 °C lower than are typically seen in benzoxazines. For each of the three diamine chain lengths, the monomer based upon unsubstituted phenol has its peak in the polymerization exotherm at a lower temperature than any of the monomers synthesized from methyl-substituted phenol. Thus, it would appear that attaching an electron-donating methyl group to the phenol has the effect of either stabilizing the benzoxazine rings against thermal activation, or reducing the effectiveness of the phenolic

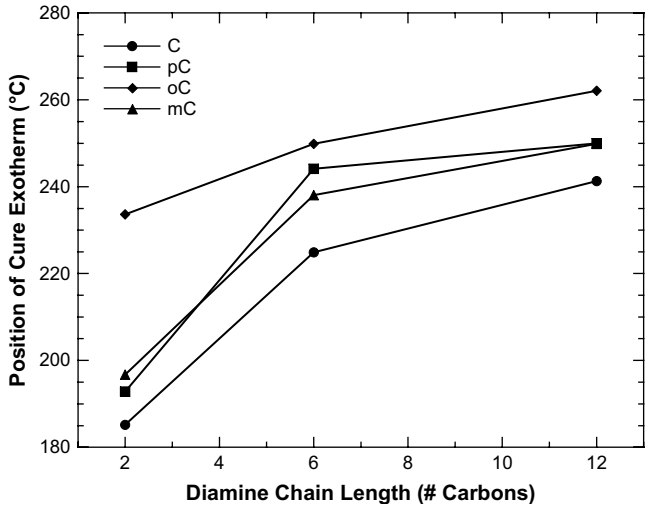

Fig. 8. Effect of phenol substitution and aliphatic diamine chain length on the position of the polymerization exotherm for the series of benzoxazine monomers.

–OH groups of open rings as initiators or catalysts. For the *o*-cresol based monomers, a methyl group blocks the preferred *ortho* reaction site, and polymerization is forced to proceed through the less favorable *para* position. As could be anticipated, these monomers require the highest temperatures to undergo polymerization for each of the diamine chain lengths.

The overlap occurring between the curing and degradation peaks in the DSC thermograms for the ethylene diamine-based monomers, as well as a few other compounds, complicates analysis of the heat of reaction for polymerization. However, this heat of polymerization can be extracted from the combined curing and degradation exotherm through careful peak fitting analysis, an example of which is shown in Fig. 9 where the exotherm of pC-ad2 monomer is resolved with three mixed Gaussian–Lorentzian peaks. Polymerization exotherms for each of the aliphatic diamine-based monomers have been calculated from the DSC thermograms, normalized to molecular weight, and are summarized in Table 2. It is quite noteworthy that, with the exception of P-ad2, each monomer has a heat of polymerization within a few percent of 100 kJ/mol regardless of phenol substitution or diamine chain length. Thus, it appears for these compounds that the mechanism and extent of benzoxazine ring opening and propagation are largely independent of both the amine length and the position on the phenolic benzene ring at which polymerization proceeds. Perhaps again due to a unique spatial or structural arrangement, the P-ad2 monomer polymerizes with a significantly higher exotherm, suggesting a different reaction mechanism than the rest of the aliphatic diamine-based benzoxazine monomers.

3.4. Kinetics of polymerization

The effect of phenol substitution and diamine chain length on the polymerization kinetics of this benzoxazine monomer series was also investigated through infrared spectroscopy. Polymerization of the monomer at 180 °C was continuously monitored using a heated transmission cell placed within the spectrometer. The benzoxazine-related absorbance peaks located between approximately 875 cm^{-1} and 965 cm^{-1} are consumed during the ring-opening polymerization. Because this absorbance band does not have any significant overlapping peaks, the fraction of oxazine rings that have been opened during polymerization can be calculated from the change in area of this benzoxazine ring mode. Without an added initiator, a benzoxazine monomer relies on the thermal activation of the oxazine ring to produce the phenolic species required to activate the autocatalytic polymerization reaction [19]. If it is assumed that Mannich bridge formation takes place following ring opening [4], then the area changes of this absorbance band can be used as an indicator of extent of reaction, such that the extent of reaction at any time, t, is given by the equation, $\alpha_t = (A_0 - A_t)/A_0$.

The fraction of the benzoxazine ring mode consumed as a function of reaction time at 180 °C is presented in Figs. 10–12 for each of the ad2, ad6, and ad12 subgroups, respectively. The polymerization kinetics of the ad2 series of monomers appears to be largely a reflection of the peak position for polymerization exotherm determined by DSC. The polymerization of the P-ad2 and pC-ad2 monomers proceeds very rapidly, reaching 50% conversion within 5 and 8 min respectively, while the reaction of oC2 appears to be delayed by a long induction time and a slower initial reaction that does not reach 50% conversion until almost 50 min. Riess et al. observed similar differences in the rate of polymerization between *ortho* and *para*-substituted monomers in a study investigating the reaction kinetics of monofunctional model compounds [12]. The polymerization of the middle diamine length monomers, P-ad6 and pC-ad6, proceeds more slowly than their shorter diamine

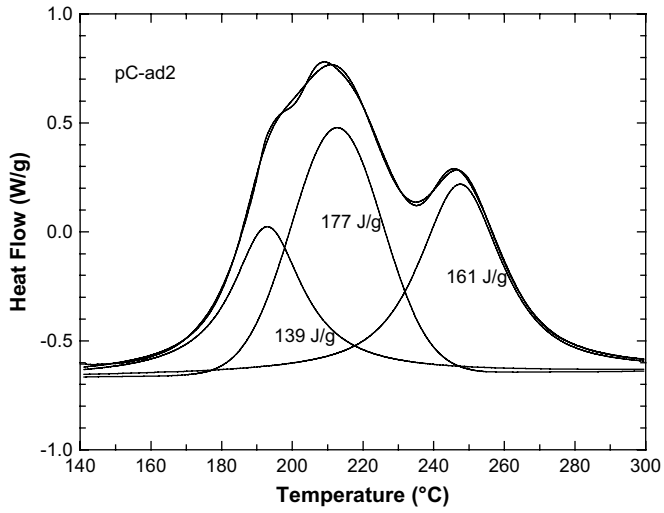

Fig. 9. Peak fitting analysis to separate the polymerization and degradation exotherms of pC-ad2.

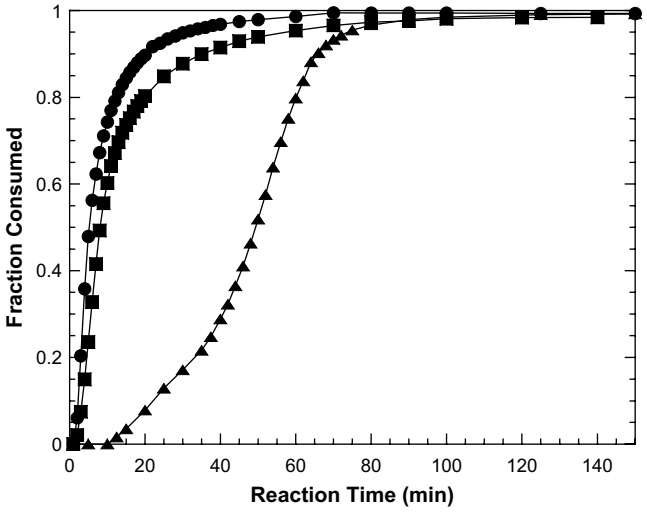

Fig. 10. Conversion of the ethylene diamine-based monomers, P-ad2 (●), pC-ad2 (■), and oC-ad2 (▲) during polymerization at 180 °C in the infrared spectrometer.

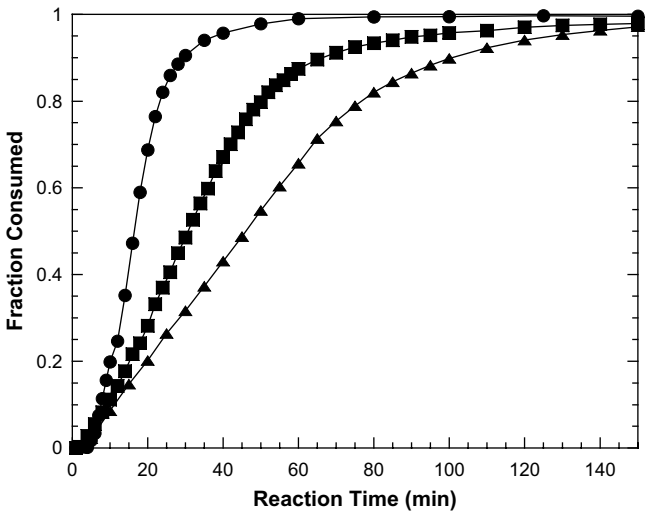

Fig. 11. Conversion of the diaminohexane-based monomers, P-ad6 (●), pC-ad6 (■), and oC-ad6 (▲) during polymerization at 180 °C in the infrared spectrometer.

counterparts, reaching 50% conversion at approximately 16 and 32 min, respectively. For this chain length, the blocked *ortho* position of oC-ad6 does not cause the induction delay seen in oC-ad2, as the reaction begins almost immediately and with a similar initial rate of reaction, reaching 50% conversion within 46 min. The reactions of monomers based on ad12, the longest diamine, continue the trend of reaction rate decreasing as the aliphatic diamine chain grows longer. In this instance, the unsubstituted compound, P-ad12, experiences an induction time of several minutes before the reaction begins to proceed rapidly, reaching 50% conversion after approximately 29 min. The *para* and *ortho*-substituted monomers, pC-ad12 and oC-ad12, polymerize at a rate very similar to their ad6 counterparts, reaching 50% conversion at 35 min and 48 min, respectively.

3.5. Infrared analysis of polymer

An infrared spectrum was also obtained for each of the cured diamine-based polybenzoxazines that were formed during the kinetic experiments. These spectra are grouped by diamine chain length and are presented in Figs. 13–15. For each polymer, the absorbance bands associated with the closed oxazine ring have completely disappeared, including those contributed from the stretching modes of the aromatic ether between 1030 and 1040 cm^{-1} and between 1221 and 1228 cm^{-1}, as well as those characteristic of the benzoxazine structure between 910 and 940 cm^{-1}.

Qualitative information about the participation of the *ortho* and *para* reactive positions during the polymerization of these benzoxazines can be obtained by examining the benzene modes in the infrared spectra. Prior to thermal reaction, the *ortho*-substituted monomers contain 1,2,3-trisubstituted benzene, while the *para*-substituted derivates possess 1,2,4-trisubstitution. However, the polymeric structure of both of these benzoxazines should exclusively contain 1,2,3,5-tetrasubstituted benzene groups, which is confirmed by the 1400–1700 cm^{-1} regions of their very similar infrared spectra.

During the polymerization of benzoxazines, a phenolic hydroxyl group is theoretically produced for every oxazine ring that is opened. Previous research has shown that hydrogen bonding of this hydroxyl group plays an important role in the network structure of polybenzoxazines and may contribute to many of their physical and mechanical properties [4]. The hydroxyl region for each of the

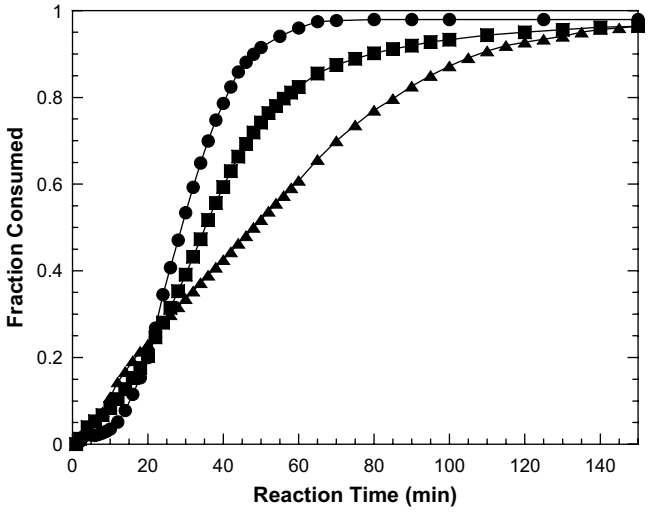

Fig. 12. Conversion of the diaminododecane-based monomers, P-ad12 (●), pC-ad12 (■), and oC-ad12 (▲) during polymerization at 180 °C in the infrared spectrometer.

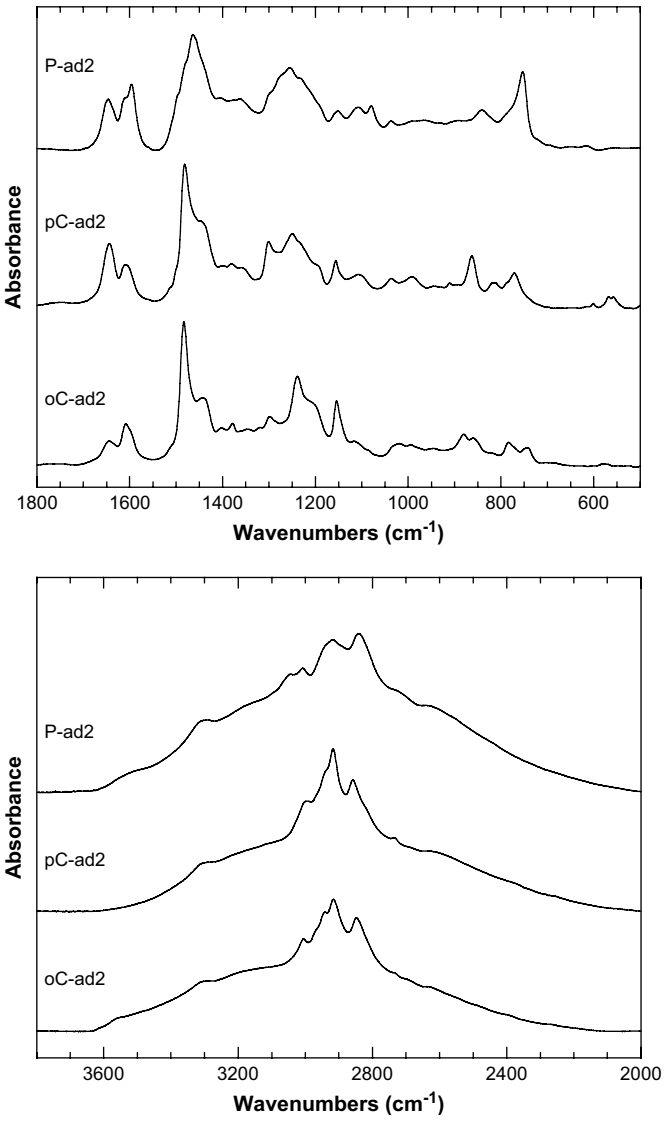

Fig. 13. Infrared spectra for the fingerprint (top) and hydroxyl regions (bottom) of the unsubstituted, *para*-, and *ortho*-substituted polymers based on ethylene diamine.

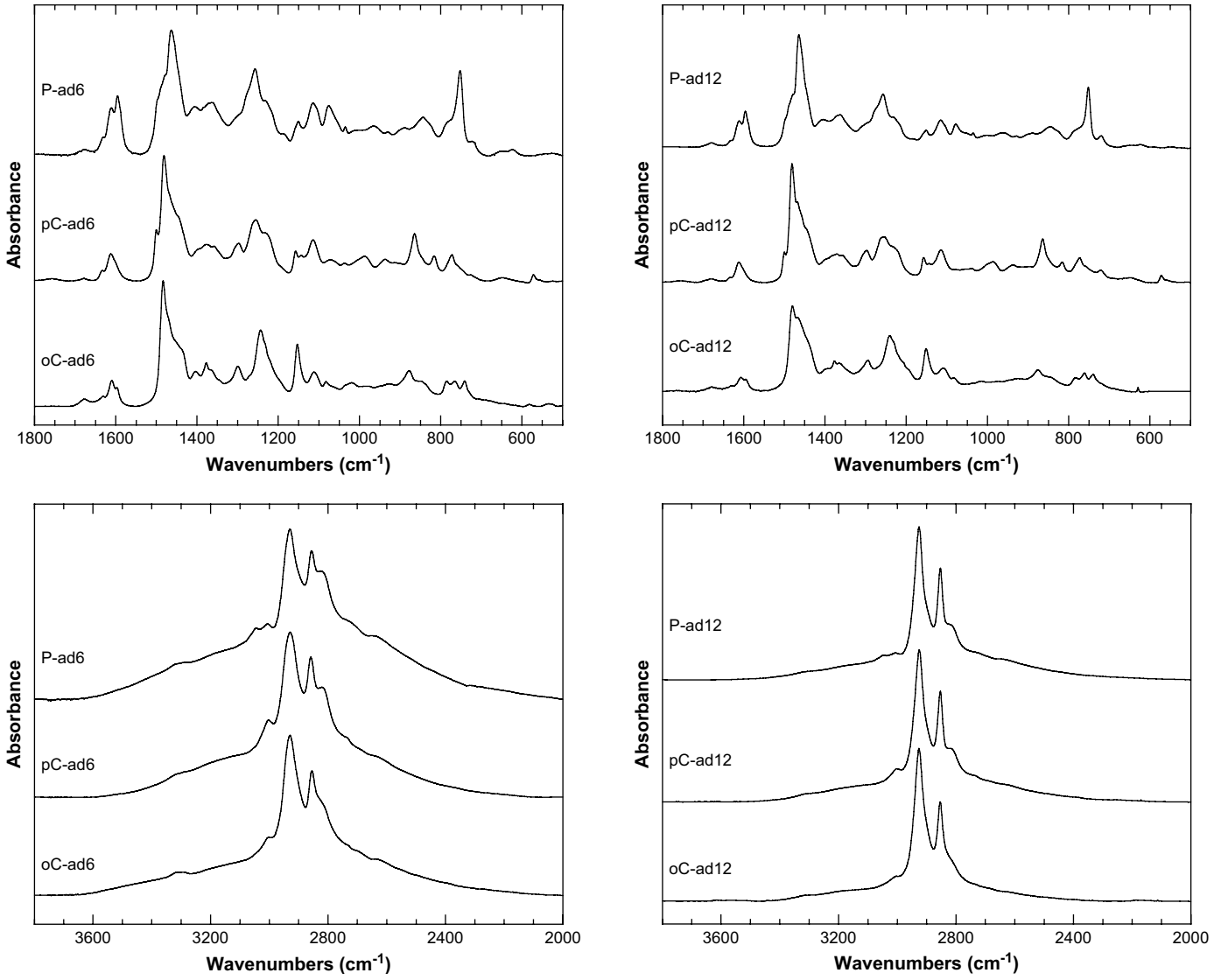

Fig. 14. Infrared spectra for the fingerprint (top) and hydroxyl regions (bottom) of the unsubstituted, *para*-, and *ortho*-substituted polymers based on diaminohexane.

Fig. 15. Infrared spectra for the fingerprint (top) and hydroxyl regions (bottom) of the unsubstituted, *para*-, and *ortho*-substituted polymers based on diaminododecane.

diamine-based polybenzoxazines is shown in the second set of polymer spectra. The absence of a peak above 3600 cm^{-1} suggests that all of the phenolic hydroxyl groups are involved in some form of intra- or intermolecular hydrogen bonding. The spectral similarities between the different polymers across this region would also seem to indicate that there is little variation in the form or type of hydrogen bonding that occurs in each polymer network. However, notably absent from the spectra of the *para*-substituted polybenzoxazines is the intramolecular absorption band appearing near 3530 cm^{-1}, which can be assigned to –OH···π hydrogen bonding [20].

3.6. Gelation phenomena

The evolution of viscoelastic properties during the polymerization of each monomer in the linear aliphatic diamine-based series of benzoxazines was continuously monitored by dynamic mechanical analysis during isochronic polymerization at 180 °C. The point of gelation for each benzoxazine was defined as the time at which the evolving dynamic storage (G') and loss (G'') moduli intersect during the isothermal polymerization experiment. While the "crossover" method of gel point determination is widely accepted [21,22], it fails in most instances to satisfy the requirements for determining true chemical gelation as defined by Winter's Gel Equation [23]. However, previous rheological analysis of bisphenol-based benzoxazines during polymerization [24] suggests that the crossover method is sufficiently accurate to estimate the vicinity of gelation for these materials.

The development over time of the viscoelastic properties of the diamine-based benzoxazines during polymerization at 180 °C is graphically presented in Figs. 16–18. The viscosities of this series of benzoxazine monomers are very low at the polymerization temperature, and do not rise beyond the threshold of measurability for the instrumentation used in this study until just a minute or two prior to gelation, at which time the viscosity rises very rapidly. Table 3 summarizes the gelation times for this series of benzoxazine monomers, as estimated by the $G' - G''$ moduli crossover point. The unsubstituted, phenol-based materials reach the point of gelation rather quickly, with a gel time that increases with the length of the aliphatic diamine chain. The P-ad2, P-ad6, and P-ad12 benzoxazines achieve a gelled state within approximately 4, 11, and 22 min respectively. All three of these materials react to form an infinite network dramatically faster than BA-a, which is reported to require more than 60 min to achieve gelation at this polymerization

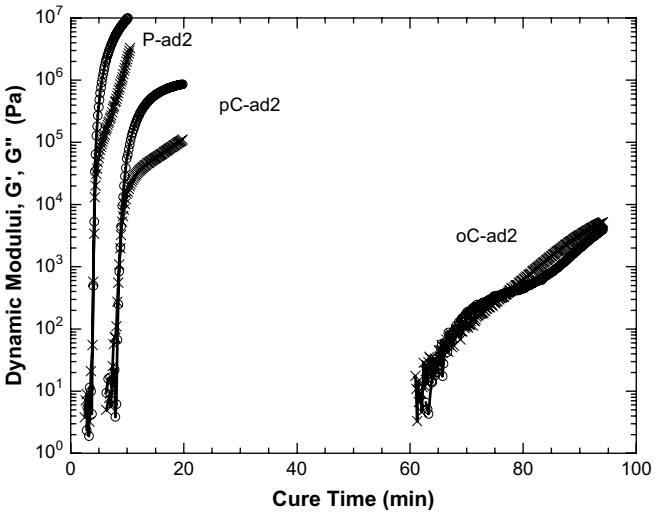

Fig. 16. Evolution of the dynamic moduli, G' (μ), and G'' (×), of the P-ad2, pC-ad2, and oC-ad2 benzoxazine monomers during polymerization at 180 °C.

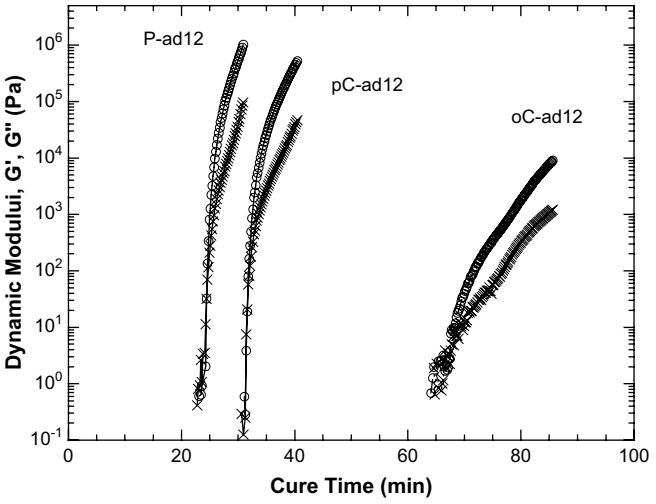

Fig. 18. Evolution of the dynamic moduli, G' (μ), and G'' (×), of the P-ad12, pC-ad12, and oC-ad12 benzoxazine monomers during polymerization at 180 °C.

temperature [24]. BA-a is a bisphenol/aniline-based material that has been widely studied and is now generally accepted as the standard reference benzoxazine. The addition of a methyl substituent to the benzoxazine monomer delays the appearance of gelation for each diamine chain length, with a blocked *ortho* position providing a greater retardation than when the *para* position is substituted.

The rheological analysis of polymerization can be combined with the kinetic results from infrared spectroscopy to determine the extent of reaction for each benzoxazine compound at its point of gelation, which is shown in Table 3. The benzoxazines from the shortest diamine, ad2, require higher conversions to reach gelation than either of their longer diamine chain counterparts with similar phenol substitution. Perhaps again related to its compact structure and potential for steric hindrance, the ad2-based benzoxazines potentially have a higher percentage of terminal branching than the longer diamine compounds, and thus require a higher degree of conversion in order to first achieve an infinite network. The P-ad6 and P-ad12 benzoxazines have very similar conversions at gelation of approximately 25%, while those of pC-ad6 and pC-ad12 are also very similar to one another at just over 40% conversion at gelation. This implies that the network growth mechanism is identical within each pair and that very similar structures are developing. While the time required to achieve the gelled state may differ, the number of reacted molecules and the types of branches and crosslinks that are formed should be similar. Within these pairs at gelation, the length of the aliphatic diamine chain will be the primary structural difference, which should manifest itself not as differences in the extent of reaction but rather in the modulus of the polybenzoxazine at the point of gelation. Unfortunately, a significant amount of air entrapped during the testing of the ad6 compounds prevents this hypothesis from being verified at this time.

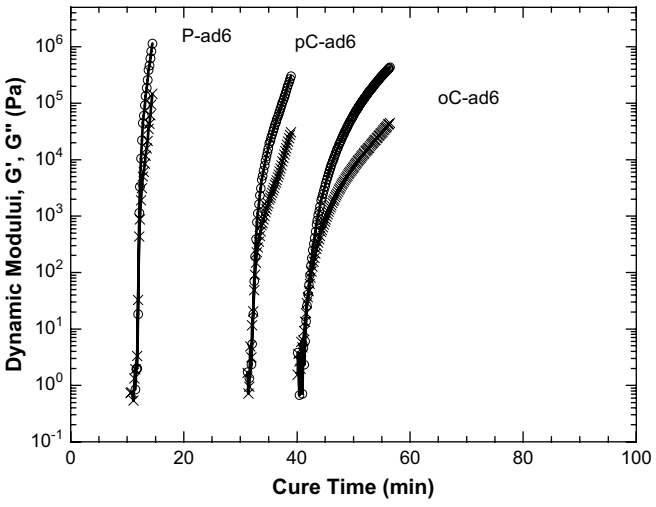

Fig. 17. Evolution of the dynamic moduli, G' (μ), and G'' (×), of the P-ad6, pC-ad6, and oC-ad6 benzoxazine monomers during polymerization at 180 °C.

3.7. Dynamic mechanical analysis

The effect of phenol substitution and aliphatic chain length on dynamic mechanical properties was also investigated for polymerization-optimized polymers prepared from this series of diamine-based benzoxazines. The dynamic storage and loss moduli, G' and G'', are grouped by diamine chain length and presented in Figs. 19–21. As can be clearly seen by comparing these figures, the sub-T_g dynamic mechanical properties of these polymers are much more strongly influenced by the length of the aliphatic diamine chain than they are by the different types of phenol substitution. The similar low temperature properties for the different substitutions within a given chain length are not surprising, since the general local structure is also expected to be

Table 3
Gelation time and conversion at gelation for each of the aliphatic diamine-based benzoxazine monomers polymerized at 180 °C.

Monomer	Gel time temperature (min)	Conversion at gelation (%)
P-ad2	4.0	36
pC-ad2	8.9	55
oC-ad2	65.4	89
P-ad6	11.0	24
pC-ad6	31.3	41
oC-ad6	41.8	45
P-ad12	22.1	28
pC-ad12	31.7	42
oC-ad12	68.0	68

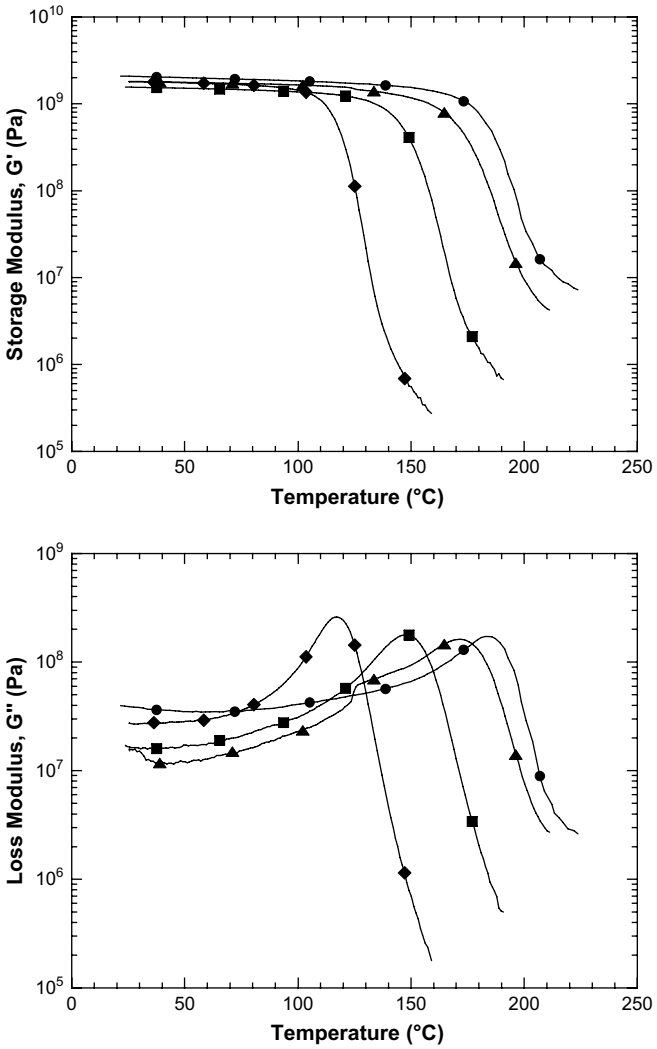

Fig. 19. Storage (top) and loss (bottom) moduli as a function of temperature for the ad2 series of aliphatic diamine-based polybenzoxazines, including P-ad2 (●), pC-ad2 (■), oC-ad2 (◆), and mC-ad2 (▲).

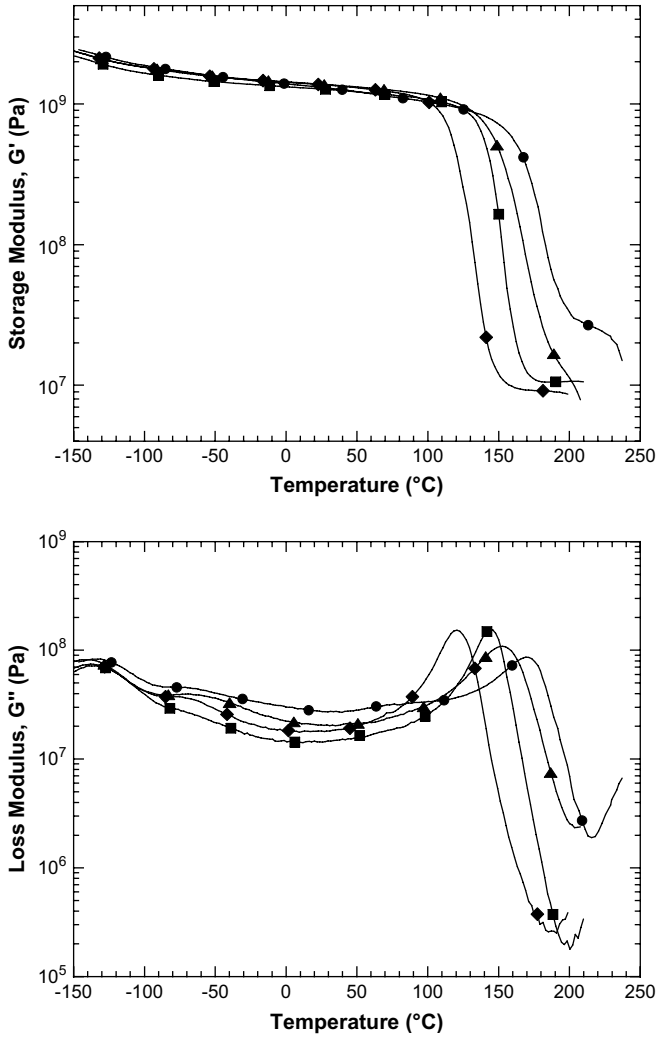

Fig. 20. Storage (top) and loss (bottom) moduli as a function of temperature for the ad6 series of aliphatic diamine-based polybenzoxazines, including P-ad6 (●), pC-ad6 (■), oC-ad6 (◆), and mC-ad6 (▲).

rather similar. The *para*-substituted polymers do, however, seem from Fig. 22 to have a lower modulus of elasticity at room temperature than any of the other substitutions. These *para*-substituted polymers were also shown by infrared spectroscopy to possess a somewhat lower degree of hydrogen bonding compared to the other substitutions. Since hydrogen bonding has been shown to play an important role in the properties of polybenzoxazines [4,18], it is likely that the elastic modulus is influenced by this lower lever of hydrogen bonding.

The glass transition temperature of each of the linear aliphatic diamine-based polymers can be determined from the maximum peak of the loss modulus, G'', and is presented for this series in Fig. 22. As noted in previous work, the unsubstituted polymers have surprisingly high glass transition temperatures when the flexible nature of the multifunctional amine core molecule is taken into consideration [18]. However, once either the *ortho* or *para* reactive site on the phenol is blocked, glass transition temperatures drop dramatically, especially for the *ortho*-substituted compounds in which the methyl group is blocking the primary polymerization site. The *meta*-substituted compounds should have a similar electron density within the benzene ring as the *ortho* and *para*-substituted compounds, but without blocking either of the two primary reaction sites. Thus, the *m*-cresol based polymers have intermediate glass transitions that are consistently 10–20 °C below the unsubstituted compounds, but well above those of the *ortho* and *para*-substituted benzoxazines.

The crosslink density of a thermosetting resin may be estimated from the plateau of the elastic modulus in the rubbery state using an equation from the statistical theory of rubber elasticity [25]:

$$G_e = \phi \upsilon RT = \phi(\rho/M_c)RT$$

where G_e is the equilibrium shear modulus in the rubbery region, ϕ is a front factor, which is unity for ideal rubbers, R is the gas constant, and T is absolute temperature. The crosslink density or concentration of network chains, υ, is the number of moles of network chains per unit volume of the polymerized polymer. If the density of the polymer, ρ, is known, then the molecular weight between crosslinks, M_c, may also be calculated. However, this equation is strictly valid only for lightly crosslinked materials and, therefore, can only be used to qualitatively compare the level of crosslinking among the various diamine-based polybenzoxazines and for comparison to other thermosets, which have reported values that were calculated in a similar manner.

As can be readily observed in the plots of storage modulus, none of the various substitutions in the ad2 series of polybenzoxazines exhibited a plateau modulus above T_g. Analysis of crosslink densities for unsubstituted and *meta*-substituted compounds in this and

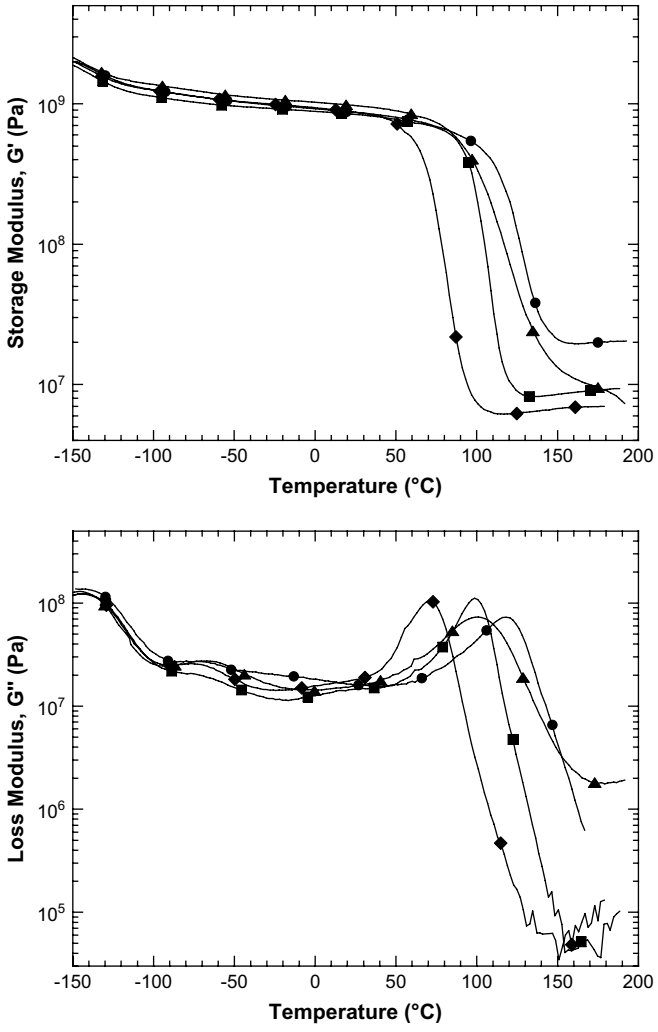

Fig. 21. Storage (top) and loss (bottom) moduli as a function of temperature for the ad12 series of aliphatic diamine-based polybenzoxazines, including P-ad12 (●), pC-ad12 (■), oC-ad12 (◆), and mC-ad12 (▲).

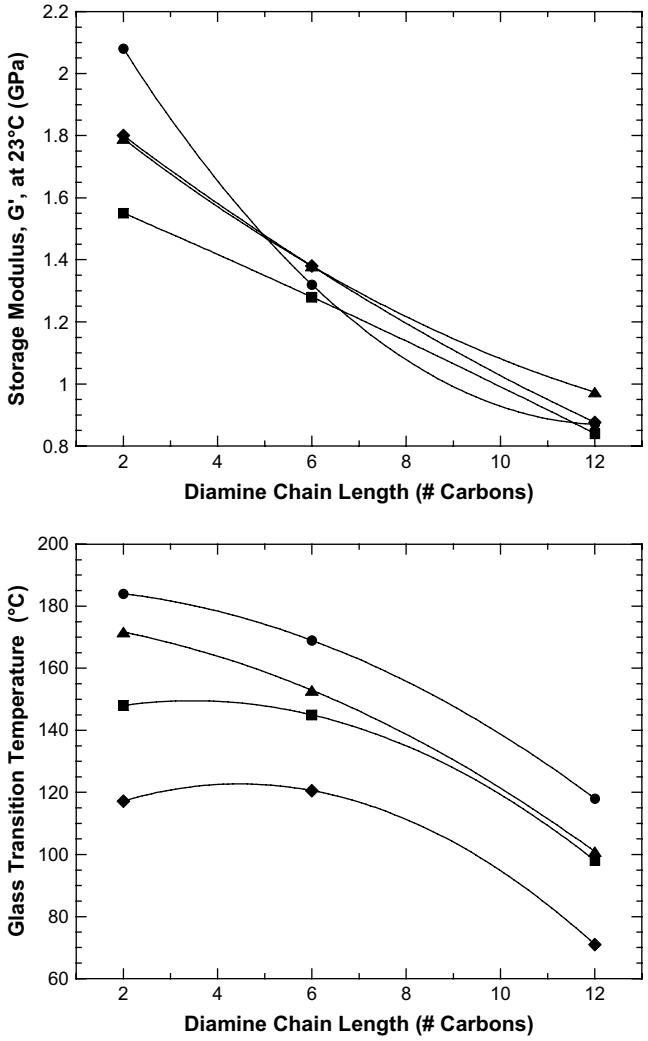

Fig. 22. Effect of phenol substitution and aliphatic diamine chain length on the room temperature storage modulus (top) and the glass transition temperature of the benzoxazine polymers: P-ad (●), pC-ad (■), oC-ad (◆), mC/ad (▲).

the ad6 series of polybenzoxazines is complicated by thermal degradation above their high glass transition temperatures. However, this does not provide an adequate explanation for the absence of a plateau in the pC-ad2 and oC-ad2 polymers, which should have sufficiently low glass transitions to avoid interference with degradation. A potentially related observation worth noting is that each of the substituted compounds in this series produced very fragile polymer specimens, brittle to the point that obtaining DMA spectra proved to be quite challenging. The ability of these materials to form high molecular weight, three-dimensionally crosslinked materials with good mechanical integrity may have been compromised by a combination of reduced monomer reactivity caused by the methyl substituent, the blocking of potential polymerization sites, and the addition of a bulky side group to a monomer structure that is already very sterically and structurally hindered.

While the P-ad6 polymer also appears to suffer from degradation in the plateau region, it is delayed just long enough to obtain a rough estimate for the value of the rubbery modulus. None of the *meta*-substituted compounds, however, exhibit a stable plateau modulus, possibly due to steric interference during polymerization caused by the close proximity of the methyl group positioned adjacent to the *ortho* reaction sites that are assumed to provide the primary path of network growth. Thus, an analysis of crosslink density will have to be limited to the unsubstituted, *ortho*-substituted, and *para*-substituted polybenzoxazines from the ad6 and ad12 diamines. The results of these calculations and the values of the plateau moduli from which they were obtained are summarized in Table 4.

It appears by the values estimated from the theory of rubber elasticity that the *ortho–ortho* linked networks of the *para*-substituted polymers have slightly higher degrees of crosslinking than the *ortho–para* network structures formed by the *ortho*-substituted polybenzoxazines. This is true for both the ad6 and the ad12 materials. Given that the benzoxazine polymerization is assumed to highly favor a reaction at the *ortho* position of the

Table 4
Summary of the results from dynamic mechanical analysis and crosslink density calculations for the linear aliphatic diamine-based series of polybenzoxazines.

Polymer	MW (g/mol)	T_g (°C)	G' at $T_{g+50\,°C}$ (MPa)	X-link density ($\times 10^{-3}$ mol/cm^3)	Mc (g/mol)	X-links per repeat unit
P-ad6	352.47	169	28.5	7.13	162	2.18
pC-ad6	380.52	145	10.6	3.05	378	1.01
oC-ad6	380.52	121	9.26	2.83	407	0.93
P-ad12	436.63	118	19.8	5.40	200	2.18
pC-ad12	464.68	99	8.49	2.75	393	1.18
oC-ad12	464.68	71	6.20	2.17	498	0.93

Table 5
Summary of the thermogravimetric analysis results for the linear aliphatic diamine-based series of polybenzoxazines.

Polymer	1% Wt. loss temperature (°C)	5% Wt. loss temperature (°C)	Char yield (%)
P-ad2	254	291	40.5
pC-ad2	241	251	17.6
oC-ad2	244	258	18.9
mC-ad2	241	273	24.0
P-ad6	266	280	18.5
pC-ad6	273	283	9.4
oC-ad6	259	277	14.0
mC-ad6	249	272	15.8
P-ad12	272	286	5.7
pC-ad12	252	287	2.0
oC-ad12	272	290	2.0
mC-ad12	255	281	4.1

phenol, it would be natural to expect the network of the unsubstituted, phenol-based polymers to consist primarily of *ortho–ortho* linkages, and be similar in structure to the network formed from the monomers with a blocked *para* position. However, a comparison between the crosslink densities of the unsubstituted, phenol-based polybenzoxazines and their *para*-substituted counterparts strongly suggests that the network structures are not as similar as may be expected. The unsubstituted polymers, P-ad6 and P-ad12, have crosslink densities that are 2–3 times greater than those of their substituted counterparts and thus can be hypothesized to have a significant number of phenol units within the network structure that are linked simultaneously at both the *ortho* and the *para* positions.

3.8. Thermogravimetric analysis

Degradation plays an important role in the optimization of curing conditions for the linear aliphatic diamine-based series of polybenzoxazines as well as interfering with the estimation of crosslink density, as discussed earlier. The results of a thermogravimetric analysis of the diamine-based polybenzoxazines are summarized in Table 5, while the weight loss and derivative weight loss curves for the ad2, ad6, and ad12 series are presented in Figs. 23–25, respectively. From the derivative weight loss curves, as well as the temperature at 1% weight loss, it is apparent that diamine chain length has a significant influence on the onset temperature for thermal degradation in a nitrogen atmosphere. From this data, it appears that with the exception of pC-ad12, thermal stability increases while the char yield systematically decreases with

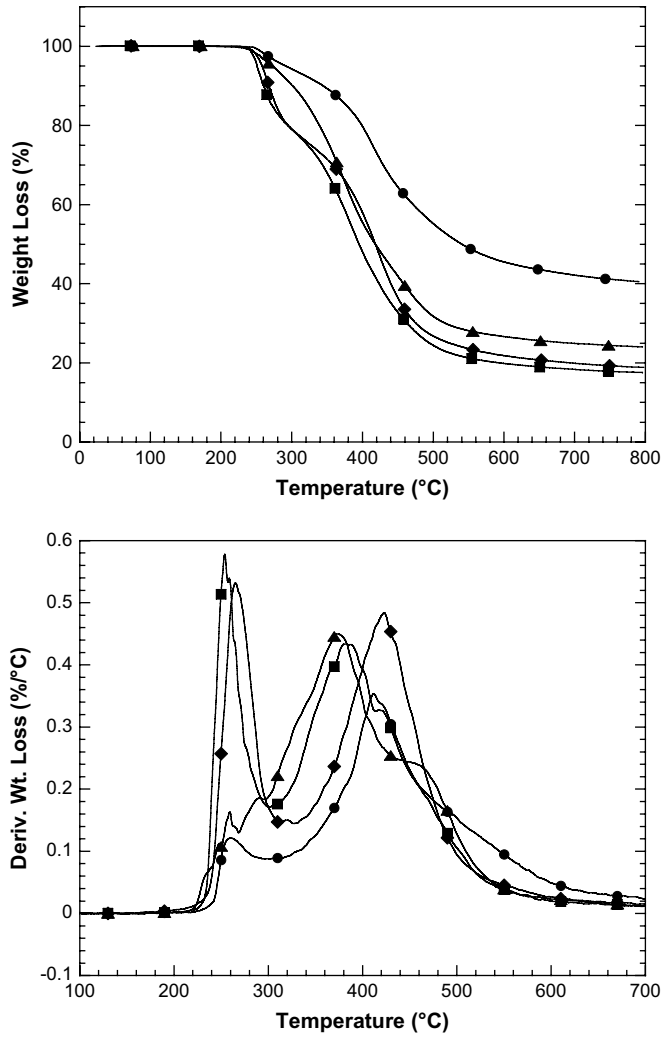

Fig. 23. Percent weight loss (top) and derivative weight loss (bottom) for the P-ad2 (●), pC-ad2 (■), oC-ad2 (◆), and mC-ad2 (▲) polybenzoxazines during thermogravimetric analysis in a nitrogen environment.

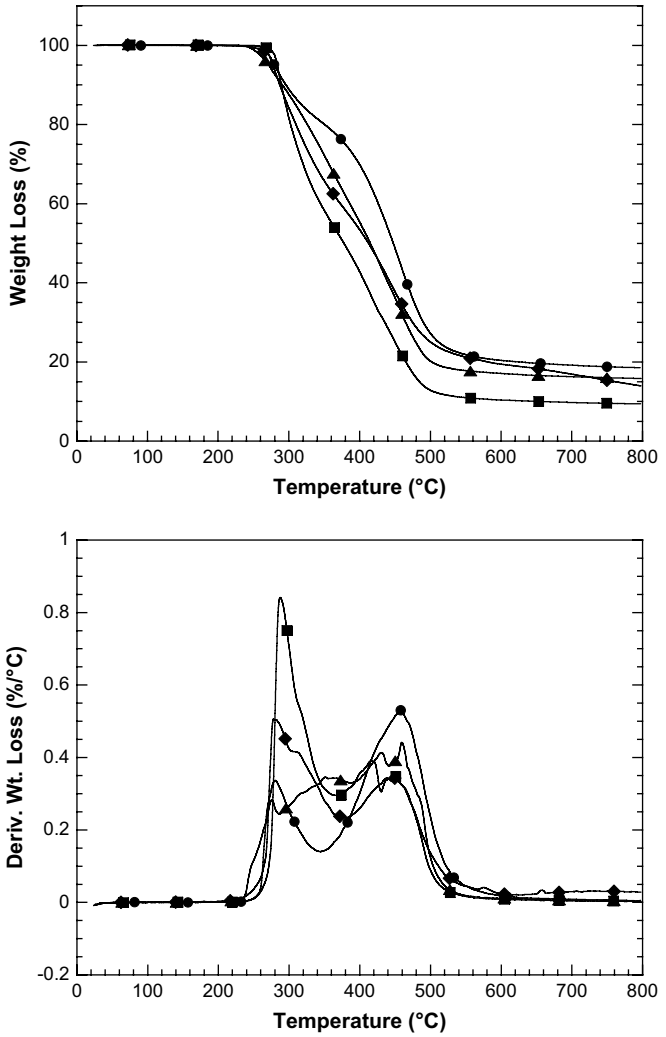

Fig. 24. Percent weight loss (top) and derivative weight loss (bottom) for the P-ad6 (●), pC-ad6 (■), oC-ad6 (◆), and mC-ad6 (▲) polybenzoxazines during thermogravimetric analysis in a nitrogen environment.

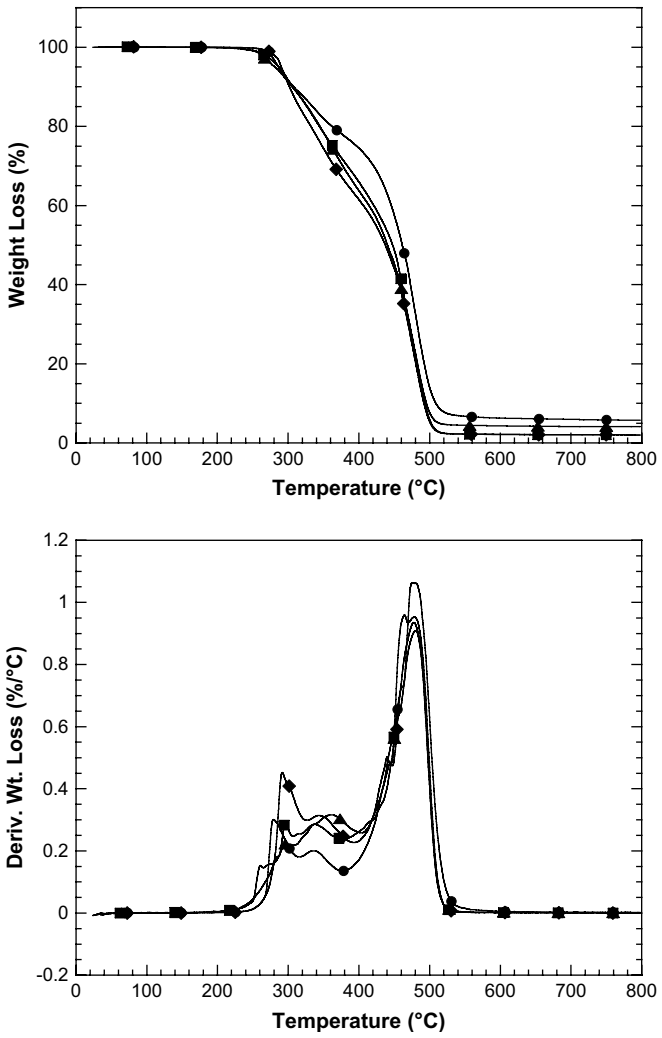

Fig. 25. Percent weight loss (top) and derivative weight loss (bottom) for the P-ad12 (●), pC-ad12 (■), oC-ad12 (◆), and mC-ad12 (▲) polybenzoxazines during thermogravimetric analysis in a nitrogen environment.

aliphatic diamine chain length for each of the different types of phenol substitution. Methyl substitution at the *ortho*, *para*, or *meta* position of these benzoxazines seems, in general, to adversely affect both the onset of degradation and the char yield. For each diamine, the *meta*-substituted compounds are among the earliest to begin thermal degradation, but perhaps because they can react at both the *ortho* and the *para* positions, have higher char yields than the other methyl-substituted polybenzoxazines.

4. Conclusions

A series of aliphatic diamine-based benzoxazines with different phenolic substitutions were successfully synthesized and characterized. The melting point of the aliphatic diamine-based benzoxazines was shown by DSC to be strongly influenced by both phenol substitution and diamine chain length. Methyl substitution decreased the reactivity of the monomer and caused the position of the polymerization exotherm to increase to higher temperatures. The normalized polymerization exotherm was largely independent of phenol substitution and diamine chain length, implying that the mechanism and extent of polymerization were similar for the majority of the monomers.

Infrared spectroscopy provided quantitative information about the reaction kinetics of the aliphatic diamine-based series of benzoxazines. The rate of polymerization for these benzoxazines decreased as a function of chain length. Phenol substitution also had the effect of slowing the polymerization process, with the reaction rate highest for the unsubstituted benzoxazines, followed by *para* substitution, and then slowest for *ortho*-substitution.

Structural analysis of the polymer by certain characteristic frequencies in the infrared spectrum suggested the successful control of the network structure. The infrared spectra provided some circumstantial evidence that both the preferred *ortho* and the less favored *para* position participated in the polymerization reaction. The *para*-substituted compounds also appear to lack the –OH$\cdots\pi$ bonding found in the rest of the polymers.

The results of the rheological gelation study mirrored those of the infrared study. Substitution was observed to delay gelation over the unsubstituted phenol-based monomers, with *o*-substituted monomers reaching gelation the slowest. Gelation times for the unsubstituted materials were much faster at 180 °C than the most common bisphenol-a based material, BA-a. The conversion at gelation was very low for the unsubstituted benzoxazines, at about 25% for P-ad6 and P-ad12, and once beyond the ad2 diamine, appeared to be independent of diamine chain length. As reaction sites were blocked, the conversion required to achieve an infinite network increased significantly.

Diamine chain length more strongly influenced the sub-T_g dynamic mechanical properties of the aliphatic diamine-based series of polybenzoxazines than phenol substitution. However, the glass transition temperature itself was significantly decreased by phenol substitution. Individually blocking either the preferred or the less favored reaction site decreased the crosslink density to roughly half of its value in the unsubstituted polymers.

Acknowledgment

The authors gratefully acknowledge the financial support of Sekisui Integrated Research.

References

[1] Burke WJ, Bishop JL, Glennie ELM, Bauer Jr WN. J Org Chem 1965;30:3423.
[2] Schreiber H. German Offen., 2,225,504; 1973.
[3] Ning X, Ishida H. J Polym Sci Part A Polym Chem 1994;32:1121.
[4] Ishida H, Allen DJ. J Polym Sci Part B Polym Phys 1996;34:1019.
[5] Kimura H, Matsumoto A, Hasegawa K, Fukuda A. J Appl Polym Sci 1999; 72:1551.
[6] Agag T, Takeichi T. Polymer 2000;41:7083.
[7] Takeichi T, Agag T, Zeidam R. J Polym Sci Part A Polym Chem 2001;39:2633.
[8] Agag T, Takeichi T. Macromolecules 2001;34:7257.
[9] Su YC, Chang FC. Polymer 2003;44:7989.
[10] Agag T, Takeichi T. Macromolecules 2003;36:6010.
[11] Lee YJ, Kuo SW, Su YC, Chen JK, Tu CW, Chang FC. Polymer 2004;45:6321.
[12] Riess G, Schwob JM, Guth G, Roche M, Lande B. In: Culbertson BM, McGrath JE, editors. Advances in polymer synthesis. New York: Plenum Press; 1985. p. 27–49.
[13] Russel VM, Koenig JL, Low HY, Ishida H. J Appl Polym Sci 1998;70:1401.
[14] Ishida H. US Patent 5,543,516; 1996.
[15] Allen DJ, Ishida H. J Appl Polym Sci 2006;101:2798.
[16] Dunkers J, Ishida H. Spectrochim Acta 1995;51A:1061.
[17] Colthup NB, Daly LH, Wiberly SE. Introduction to infrared and Raman spectroscopy. 3rd ed. New York: Academic; 1990.
[18] Allen D, Ishida H. Polymer 2007;48:6763.
[19] Dunkers J, Ishida H. J Polym Sci Part A Polym Chem 1913;37:1999.
[20] Cairns T, Eglinton G. J Chem Soc 1965:5906.
[21] Tung CYM, Dynes PJ. J Appl Polym Sci 1982;27:569.
[22] ASTM D4473-90. Measuring the cure behavior of thermosetting resins using dynamic mechanical procedures; 1990.
[23] Winter HH. Polym Eng Sci 1987;27:1698.
[24] Ishida H, Allen DJ. J Appl Polym Sci 2001;79:406.
[25] Treloar LRG. The physics of rubber elasticity. London: Oxford University Press; 1949. p. 66.